IEEE Access
Multidisciplinary ⋮ Rapid Review ⋮ Open Access Journal

Received January 28, 2021, accepted February 1, 2021, date of publication February 10, 2021, date of current version February 17, 2021.

Digital Object Identifier 10.1109/ACCESS.2021.3058589

Stochastic Optimal Planning of Distribution System Considering Integrated Photovoltaic-Based DG and DSTATCOM Under Uncertainties of Loads and Solar Irradiance

EYAD S. ODA[1], AMAL M. ABD EL HAMED[2], ABDELFATAH ALI[3], ADEL A. ELBASET[4,5], MONTASER ABD EL SATTAR[3], AND MOHAMED EBEED[6]

[1]Department of Electrical Engineering, Faculty of Engineering, Suez Canal University, Ismailia 41522, Egypt
[2]Electricity Department, Faculty of Technology and Education, Sohag University, Sohag 82524, Egypt
[3]Department of Electrical Engineering, Faculty of Engineering, South Valley University, Qena 83523, Egypt
[4]Electrical Engineering Department, Faculty of Engineering, Minia University, Minya 61519, Egypt
[5]EL-Arish High Institute of Engineering and Technology, Arish 45511, Egypt
[6]Department of Electrical Engineering, Faculty of Engineering, Sohag University, Sohag 82524, Egypt

Corresponding author: Eyad S. Oda (eyad.oda@eng.suez.edu.eg)

ABSTRACT Optimal planning of integration the Photovoltage Distributed Generation (PV-DG) and DSTATCOM is a crucial task due to the stochastic variations of PV output power and the load demand which are related to solar irradiance variations and the activities of the customers, respectively. In this article, the optimal planning problem of the PV-DG and DSTATCOM system is solved. The proposed model considers the uncertainties of the solar irradiance and the load demand for a multi-objective function, including the cost reduction, the voltage profile, and stability index improvement. Modified Ant Lion Optimizer (MALO) is proposed to enhance the basic ALO searching ability using two strategies. The first strategy is based on Levy Flight Distribution (LFD) to strengthen the exploration of the algorithm and avoid the premature of the basic ALO. In contrast, the second strategy is based on updating the solutions in a spiral orientation to improve the exploitation of the algorithm. The IEEE 69-bus and 118-bus radial distribution systems are used to demonstrate the effectiveness of the proposed method, and the yielded simulations are compared with the basic ALO and other well-known optimization techniques for power loss minimization under deterministic conditions. The simulation results demonstrate that the techno-economic benefits can be increased considerably by optimal inclusion of two PV-DGs and DSTATCOMs compared with a single system.

INDEX TERMS Distributed generators, PV, DSTATCOM, optimal planning, uncertainty, electrical distribution.

I. INTRODUCTION

A. LITERATURE SURVEY

Integration of renewable distributed generators and the shunt compensators is an effective solution from technical and economic perspectives. Several renewable-based technologies have been progressed to generate the required electricity, including wind turbine, biomass, solar thermal, solar PV, geothermal and hydro systems [1]. Distribution Flexible AC Transmission System(D-FACTS) are also widely embedded in the distribution grid [2]. D-FACTS include numerous controllers such as Distribution Static Var Compensator (D-SVC), unified power quality conditioner (UPQC), and Distributed static compensator (DSTATCOM) [3]. The inclusion of DGs can yield several economic, technical, and environmental benefits. It can also reduce the power loss, reduce the voltage deviation, maximize the system reliability, and decrease the emissions of greenhouse gases, dimmish the generation cost [4].

DSTATCOM is an efficient device working on a voltage source converter connected in shunt to a certain bus. DSTATCOM is better than the other shunt compensation devices;

The associate editor coordinating the review of this manuscript and approving it for publication was Qiuye Sun.

this is due to its fast response to inject or absorb reactive power through injection of a controllable voltage as well as its capability to mitigate the system harmonic, the load balance, and improving the system performance considerably. Furthermore, it has not any operational problems such as transient harmonics or resonance, unlike series or shunt capacitors [3], [5], [6].

The optimal integration of DSTATCOM in distribution grids has been presented in many papers. In [7], the immune algorithm has been employed to assign the siting and sizing of the DSTATCOM for cost and loss reduction. In [8], Harmony Search Algorithm has been implemented to optimize the site and size of the DSTATCOM for loss reduction. In [5], Differential evolution (DE) technique has been applied for optimizing the site and size of the DSTATCOM with optimal network reconfiguration for losses reduction. The binary gravitational search technique has been employed to assign the site and size of the DSTATCOM for enhancement [9]. The authors in [10] have applied the imperialist competitive algorithm to determine the optimal site and capacity of the DSTATCOM for a multi-objective function under uncertainties of the load demand. A Bio-Inspired Cuckoo Search technique has been used for optimizing the allocation of the DSTATCOM for loss reduction under different load models [11]. In [12], the whale optimization algorithm has been applied for optimizing the allocation of DSTATCOM in the distribution network. In [13], the differential evolution algorithm has been used to assign the location and size of DSTATCOM for cost and loss reduction. The site and size of the DSTATCOM are allocated to reduce the losses and boost the stability and the voltage profile using a multi-objective sine cosine Algorithm [14]. The Fuzzy-GA based algorithm has been employed to optimize the allocation of the DSTATCOM for reducing losses and the total cost [14], [15].

The motivation of using PV-DG comes from several aspects compared with other types of RERs: 1) no moving parts are needed, 2) high reliability with at least a 25-year warranty, 3) less conspicuous than a wind turbine 4) less susceptible to high wind damage and 5) requires less space in most cases as the panels can be installed on a roof 6) the mutual relationship of environment, economic and power network performance is strongly interrelated for this type. Numerous efforts have been presented to allocate the PV-DG in the power system. In [16], the optimal allocation of the PV-DG and DSTATCOM is assigned using a fuzzy approach and ant colony algorithm. The PSO has been employed to allocate the DSTATCOM and DG for reducing the losses and support the voltage [17]. The Bacterial Foraging Optimization technique has been applied to assign the DSTATCOM and DG to minimize the cost, the losses, and the voltage profile [18]. In [19], the DSTATCOM and DG allocation is solved using the lightning search algorithm for loss reduction and boosting the voltage profile and stability. In [20], the optimal PV, DSTATCOM, and energy storage unit has been assigned optimally for voltage profile and reliability improvement, and cost minimization. The authors in [21] have applied the whale optimization algorithm to optimize the sites and sizes of the DSTATCOM and DG to reduce cost and losses. In [22], the DSTATCOM and DGs allocation has been optimized the hybrid lightning search algorithm with the simplex method for reducing cost, loss, and voltage deviations. In [23] the authors applied the Harris Hawks Optimization algorithms to assign the optimal location and sizes at different values of the power factors.

Incorporating renewable distributed energy resources (RDERs) in distribution networks such as solar PV units is challenging due to seasonal and daily variations of the solar irradiance and the weather variations that increase the uncertainty in the power system. Thus, it is mandatory to consider the uncertainties of the RDERs for efficient planning in the power system. Several efforts have been presented to integrate the DGs under the uncertainties. In [24], the optimal planning problem has been solved with RDERs considering uncertainties of solar radiation, load demand, and wind speed. The authors in [25] assigned the DGs' optimal size and site under uncertainties of the RDERs fuel price and future load growth. In [26]–[29], The optimal reactive power dispatch problem has been solved under the uncertainties of renewable sources. In [30]–[34], the optimal site and a rating of the RDERs have been assigned optimally under uncertainties of the solar radiation, wind speed, and load demand.

Ant Lion Optimizer (ALO) is an efficient technique based on the ant lion's hunting behavior. It should be highlighted here that the ALO algorithm includes the main two techniques (i.e., population-based search strategy and local-based search strategy) to produce an intelligent technique that can search effectively by the two main search strategies (global exploration and local exploitation). Compared to the other meta-heuristic methods, ALO algorithm is easy, simply implemented, and adjustable. Thus, the ALO is applied for solving the planning problem.

Thus, ALO has been employed in solving many optimization problems [35]–[37]. However, ALO succeeded in solving several optimization problems; it suffers from stagnation in some cases. Insequent, several modified and improved versions of the ALO have been emerged to enhance the searching abilities of the conventional ALO. Z. Wu *et al.* presented an improved ALO version based on chaotic sequence for assigning individual initial location for realizing the parameter of the solar PV model [38]. In [39], a modified ALO has been presented, which is based on Lévy flight to optimize the feature selection. The authors in [40] proposed a hybrid binary ALO with hill-climbing techniques for feature selection. S.K. Dinkar and K. Deep presented an opposition Laplacian ALO for Gear Train Design and Capacity of Gas Production Facilities [41]. In [42], the authors have proposed a modified version of the ALO based on the chaotic mapping approach to recognize and State of Charge evaluation of NMC Cells. S.K. Dinkar and K. Deep presented a modified version of the ALO based on opposition learning with Lévy Flight [43]. In [44], a modified ALO version is based on

chaotic maps to optimize the feature selection. The author in [45] presented a consensus algorithm with multiagent system which has been applied to distributed generators in the Energy Internet for improving and increasing the energy utilization. In [46], a line impedance cooperative stability region method for grid-tied inverters under weak grids has been presented.

It is worth mentioning that the Levy Flight Distribution (LFD) application has been proposed earlier. However, it is still applied widely to enhance the exploration of optimization algorithms where the application of the LFD enables the population to jump to new areas to avoid stagnations of the optimization algorithms [47]–[50]. Also, populations' spiral movement around the best solution is an efficient approach for enhancing the exploitation phase and search abilities of several optimization algorithms [51]–[53]. Thus, in this article, a modified Ant Lion Optimizer (MALO) is proposed for enhancing the searching ability of the basic ALO using Levy Flight Distribution (LFD) and spiral orientation of the population to strengthen the exploration and exploitation of the basic ALO.

Solving the optimal power planning in the distribution system with the DGs and the compensators has drawn researchers' attention in the last decades. Due to uncertainties of load and solar irradiance, the power planning under uncertainties in the power system becomes difficult to solve in actual implementation. To address this issue, the uncertainties of the solar irradiance and load demand have been modeled. An efficient optimization approach has been proposed and applied for solving this problem working on an improved version of the ALO.

B. CONTRIBUTION OF PAPER

It should be highlighted here that most of the presented works related to optimal allocation of DG and DSTATCOM problem have been solved at the deterministic condition or solving the optimal power planning considering the technical and the economic perspective separately. In this article, the optimal power planning problem with integration of the PV-DG and DSTATCOM has been solved considering uncertainties of the solar irradiance and load demands of four seasonal (summer, winter, spring, autumn) variations of these parameters. Besides that, an improved version of the ALO is proposed to solve the planning problem based on Levy flight distribution and spiral orientation. The main contributions are summarized as follows:

- Solving the optimal planning problem in the distribution system under optimal integration of the PV-DG and DSTATCOM.
- Considering the uncertainties of the load demand and solar radiation in four seasons based on three years of historical data.
- Proposing a modified ALO version for solving the presented problem based on two improvements includes the spiral movement around the best solution and the levy flight-based motion.
- The mathematical model of the optimal planning problem is formulated as a multi-objective optimization problem that includes the total annual cost and voltage deviations reductions and stability enhancement.
- The obtained outcomes clearly indicate that scenario 2 (Optimal installation of two-hybrid systems) is more effective in optimal planning.

C. PAPER LAYOUT

The paper is organized as follows: Section II 'Problem Formulation' described the considered objective function along with the constraints. Section III 'Uncertainty modeling' explains the strategy of considering the uncertainty of the load and the solar irradiance. Section IV 'Ant Lion Optimizer' gives an overview of the ALO. Section V 'Modified Ant Lion Optimizer' depicts the concept of the MALO. Section VI 'simulation results' shows the yielded results by application the MALO. Finally, Section VII 'Conclusion' summarizes the outcomes of the paper.

II. PROBLEM FORMULATION

A. THE OBJECTIVE FUNCTION

The main presented task of this work is maximizing the techno-economic benefits of optimal planning of integration of the PV-DG and DSTATCOM in the power system. It should be highlighted here that the planning period is carried out for three years where the uncertainity of the load demand and solar irradiance are considered in the four seasons in which each season includes 91.25 days. The objective function to be minimized is a multi-objective function including the cost reduction, the voltage profile, and stability index improvement, which can be formulated as follows:

$$min\ F = min\ (\omega_1 \times Obj_1 + \omega_2 \times Obj_2 + \omega_3 \times Obj_3) \quad (1)$$

where Obj_1, Obj_2, and Obj_3 denote cost reduction, voltage deviations minimization, and voltage stability index (VSI) enhancement, respectively. ω, ω_2, and ω_3 represent the weighting factors. Summation of the weighting factors should be formulated as follows:

$$|\omega_1| + |\omega_2| + |\omega_3| = 1 \quad (2)$$

in which:

$$Obj_1 = \frac{Cost_{With}}{Cost_{Wo}} \quad (3)$$

$$Obj_2 = \frac{TVD_{With}}{TVD_{Wo}} \quad (4)$$

$$Obj_3 = \frac{1}{\sum_{n=1}^{NB} VSI_n} \quad (5)$$

where $Cost_{Wo}$ and TVD_{WO} denote the total cost and summation voltage deviations without inclusion PV-DG or DSTATCOM, respectively. $Cost_{With}$ denotes the total annual cost, which can be formulated as follows:

$$Cost_{With} = Cost_{Loss} + Cost_{Grid} + Cost_S + Cost_{PV} \quad (6)$$

where $Cost_{Loss}$, the energy power loss, $Cost_{Grid}$, $Cost_{PV}$ and $Cost_S$ are the cost of the energy losses, the cost of the injected energy at the substation, the installation cost of the PV unit, and the installation cost of the DSTATCOM, respectively. in which

$$Cost_{Loss} = C_{loss} \times 91.25 \times \sum_{i=1}^{Ns} \sum_{h=1}^{24} \sum_{j=1}^{NT} P_{Loss(i,h,j)} \quad (7)$$

where C_{loss} denotes the cost of the energy loss. Ns equals 4, which represents the number of seasons per year. NT represents the number of the network branches. The power loss in each transmission line is given as follows:

$$P_{Loss} = R_{n,n+1} \left(\frac{P_n^2 + jQ_n^2}{|V_n|^2} \right) \quad (8)$$

The cost of the power injection at the substation which is expressed as follows:

$$C_{Grid} = C_{Grid} \times 91.25 \times \sum_{i=1}^{Ns} \sum_{h=1}^{24} P_{Grid(i,h)} \quad (9)$$

The installation cost of the DSTATCOM is expressed as follows:

$$Cost_S = C_S \times Q_S \times \frac{(1+\alpha)^{Ns} \times \alpha}{(1+\alpha)^{Ns} - 1} \quad (10)$$

where Q_S denotes the rated kVar of the DSTATCOM; C_S represents the capital cost of DSTATCOM; Ns is the lifetime of the DSTATCOM in years; α denotes the asset rate of return DSTATCOM. The installation cost of the PV system includes fixed cost ($Cost_{Fix}$) and the variable cost ($Cost_{Var}$) which can be represented as follows:

$$Cost_{PV} = Cost_{Fix} + Cost_{Var} \quad (11)$$

$$Cost_{Fix} = CR \times C_{PV} \times P_r \quad (12)$$

where C_{PV}, P_r, and CR are the purchased cost of the PV unit in \$/kW, rated power of the PV system, and capital recovery factor, which can be founded as follows:

$$CR = \frac{\tau \times (1+\tau)^{NP}}{(1+\tau)^{NP} - 1} \quad (13)$$

where τ is the rate of interest on capital investment of the installed PV; NP is the lifetime of the PV-DG in years; $Cost_{Var}$ is calculated as follows:

$$Cost_{Var} = C_{O\&M} \times \sum_{i=1}^{Ns} \sum_{h=1}^{24} P_{PV(i,h)} \quad (14)$$

where $C_{O\&M}$ denotes the operation and maintenance cost, which is associated with the output kWh of the PV unit; P_{PV} represents the output power of the PV unit, which can be given as follows:

$$P_{PV} = \begin{cases} P_r \left(\frac{G_s^2}{G_{std} \times X_c} \right) & for\ 0 < G_s \le X_c \\ P_r \left(\frac{G_s}{G_{std}} \right) & for\ X_c \le G_s \le G_{std} \\ P_r & G_{STD} \le G_s \end{cases} \quad (15)$$

where G_s and G_{std} are the solar irradiance in W/m^2 and standard solar irradiance environment, which is 1000 W/m^2, respectively. X_c represents a certain irradiance point. The second objective function is enhancing the voltage profile by diminishing the voltage deviations, which can be expressed as follows:

$$TVD = 91.25 \times \sum_{i=1}^{Ns} \sum_{h=1}^{24} \sum_{n=1}^{NB} |V_n - 1| \quad (16)$$

where TVD is the summation of voltage deviations while NB denotes the number of buses. The third considered function is enhancing the stability by maximizing the voltage stability index (VSI_n) as follows:

$$TVSI = 91.25 \times \sum_{i=1}^{Ns} \sum_{h=1}^{24} \sum_{n=1}^{NB} VSI_n \quad (17)$$

in which:

$$VSI_n = |V_n|^4 - 4\left(P_{mn+1}X_n - Q_{n+1}R_n\right)^2 - 4\left(P_{n+1}X_n + Q_{n+1}R_n\right)|V_n|^2 \quad (18)$$

B. THE SYSTEM CONSTRAINTS

1) EQUALITY CONSTRAINTS

The equality constraints represent the balanced powers as follows:

$$P_{Slack} + \sum_{i=1}^{NPV} P_{PV,i} = \sum_{i=1}^{NT} P_{loss,i} + \sum_{i=1}^{NB} P_{L,i} \quad (19)$$

$$Q_{Slack} + \sum_{i=1}^{NDS} Q_{DS,i} = \sum_{i=1}^{NT} Q_{loss,i} + \sum_{i=1}^{NB} Q_{L,i} \quad (20)$$

where P_{Slack} and Q_{Slack} are the active and the reactive powers from the substation, respectively. P_L and Q_L are the active and reactive load demands, respectively. NPV is the number of PV unit while NDS denote to number DSTATCOM in the grid.

2) INEQUALITY CONSTRAINTS

$$V_{min} \le V_i \le V_{max} \quad (21)$$

$$I_n \le I_{max,n} \quad n = 1, 2, 3 \ldots, NT \quad (22)$$

$$\sum_{i=1}^{N_{PV}} P_{PV} \le \sum_{i=1}^{NB} P_{L,i} \quad (23)$$

$$\sum_{i=1}^{NDS} Q_{DST,i} \le \sum_{i=1}^{NB} Q_{L,i} \quad (24)$$

where V_{min} is the minimum voltage limit while V_{max} represents the maximum voltage limit. $I_{max,n}$ denotes the maximum limit of current in line number n.

III. UNCERTAINTY MODELING

This section describes the uncertainty modeling of the PV and load demand. The probabilistic generations of the load demand and each PV unit have been modeled based on the location's hourly historical data under research. Three years

of hourly historical data for solar irradiance and load demand have been considered in this work. Therefore, every single year has been divided into four seasons. A day within a season (24−h) is considered for characterizing the stochastic behavior of the PV and load demand during this season. Hence, each year has 96 time periods (4 seasons× 24 − h). For each season, the probability distribution function (pdf) of each period can be obtained by utilizing the data related to the same hours of the day. Consequently, each period has 270 solar irradiances and load demand (3 years×3 months per season ×30 days per month) to generate the corresponding hourly pdfs. The probabilistic model of the PV system and load demand can be characterized as follows.

A. SOLAR IRRADIANCE MODELING

The data of the solar irradiance for each hour have been used to generate a Beta pdf for that hour and can be described as follows [44], [45]:

$$f_b(g_s) = \begin{cases} \frac{\Gamma(\alpha+\beta)}{\Gamma(\alpha).\Gamma(\beta)} g_s^{(\alpha-1)}. \quad (1-g_s)^{(\beta-1)}, 0 \le g_s \le 1; \alpha, \beta \ge 0 \\ 0, \qquad\qquad\qquad Otherwise \end{cases} \tag{25}$$

where $f_b(g_s)$ denotes the Beta pdf of the solar irradiance; Γ represents the gamma function; α and β are the Beta parameters for each period. These parameters can be determined using the historical data as follows [27], [54]:

$$\beta = (1-\mu) \times \left(\frac{\mu \times (1+\mu)}{\sigma^2} - 1 \right) \tag{26}$$

$$\alpha = \frac{\mu \times \beta}{1-\mu} \tag{27}$$

where μ and σ are the mean and standard deviation of the solar irradiance for each period. The continuous Beta pdfs are split into numerous segments where each segment generates a mean value and a probability of occurrence. The occurrence probability of a segment during a specific hour can be determined by:

$$prob_i^{g_s} = \int_{g_{s,i}}^{g_{s,i+1}} f_b(g_s)\, dg_{s,i} \tag{28}$$

where $g_{s,i}$ and $g_{s,i+1}$ represent, respectively, the start and endpoints of the interval i. $prob_i^{g_s}$ represents the probability occurrence of interval i. Based on the generated Beta pdf of the solar irradiance of a period, the output power PV for this period's states can be calculated using (15).

B. LOAD DEMAND MODELING

As the load demand has a stochastic nature, normal pdf is utilized for modeling it at each bus. The normal pdf of the uncertain load demand can be determined as follows [44]:

$$f_n(l) = \frac{1}{\sigma_l \sqrt{2\pi}} \times exp\left[-\left(\frac{l-\mu_l}{2\sigma_l^2} \right) \right] \tag{29}$$

w where $f_n(l)$ represents the normal pdf of the load demand; μ_l and σ_l represent the mean and standard deviation of the load demand for each period. The occurrence probability of a segment during a specific hour can be expressed as follows:

$$prob_i^l = \int_{l_i}^{l_{i+1}} f_n(l)\, dl \tag{30}$$

where l_i and l_{i+1} denote the starting and ending points of the interval i. $prob_i^l$ represents the probability occurrence of interval i.

C. COMBINED MODEL OF PV AND LOA

The probabilistic models of the solar irradiance and load demand given in subsections A and B are utilized to create a combined probability model ($P_{com,i}$) of PV-load. For each time period, the combined model of the interval i can be computed by convoluting the probabilities of the solar irradiance and load demand, as follows:

$$P_{com,i} = prob_i^{g_s} \times prob_i^l \tag{31}$$

For each state, the objective function given in (1) should be calculated and weighted according to the probability of occurrence (i.e., combined probability model) of this state during the whole planning period. Each time segment represents one hour. This means that each time period there are several values for each variable. However, for the sake of simplicity, we have only shown the expected or mean values of the variables.

IV. ANT LION OPTIMIZER

Ant Lion Optimizer (ALO) is a population-based optimization technique presented by Seydali Mirjalili in 2015 [35]. ALO simulates the hunting behavior of Ant Lion and the interaction between the prey or the ants and the predator ant lions where the ant lions build circular traps to hunt the ants. The ants move in a stochastic pattern to search for their foods. The mathematic model of the stochastic movement of the ants is formulated as follows:

A. RANDOM MOVEMENT OF AN ANT

The random movement of the ant is described using the following equation:

$$X(t) = [0, cumsum(2r(t_1) - 1), cumsum(2r(t_2) - 1), cumsum(2r(t_n) - 1)] \tag{32}$$

where $x(t)$ represents the location of the ant at the t-th iteration. cumsum denotes the cumulative sum. N is the maximum number of iterations. $r(t)$ denotes a random which can be given as follows:

$$r(t) = \begin{cases} 1 & if\ r\ and > 0.5 \\ 0 & if\ r\ and \le 0.5 \end{cases} \tag{33}$$

The min-max normalization equation is utilized for keeping the ants move in random walks inside the search spaces,

which can be described as follows:

$$R_i^t = \frac{\left(X_i^t - a_i\right) \times \left(U_i^t - L_i^t\right)}{d_i - a_i} + L_i \tag{34}$$

here $\boldsymbol{R_i^t}$ denotes the location of the i-th ant after random walk closed to j-th antlion. $\boldsymbol{U_i^t}$ and $\boldsymbol{L_i^t}$ are the upper and the lower boundaries of i-th variable at t-th iteration, respectively. $\boldsymbol{a_i}$ and $\boldsymbol{d_i}$ represents the minimum and the maximum steps of random walk, respectively. The ants will update their positions based on a random walk, and they will be trapped in the ant lion pit. The positions of ants are listed in a matrix as follows:

$$M_{Ant} = \begin{bmatrix} X_{1,1} & X_{1,2} & \cdots & X_{1d} \\ X_{2,1} & X_{22} & \cdots & X_{2,1} \\ \vdots & \vdots & \ddots & \vdots \\ X_{n,1} & X_{n,2} & \ldots & X_{n,d} \end{bmatrix} \tag{35}$$

The corresponding objective functions for each vector of the ant positions are listed as follows:

$$Obj_{Ant} = \begin{bmatrix} f_1\left(X_{1,1}, X_{1,2}, \ldots, X_{1d}\right) \\ f_2\left(X_{1,1}, X_{1,2}, \ldots, X_{1d}\right) \\ \vdots \\ f_n\left(X_{1,1}, X_{1,2}, \ldots, X_{1d}\right) \end{bmatrix} \tag{36}$$

The search agents (ant positions) are sorted, and the best agents are selected as antlions, which are listed as follows:

$$M_{Antlion} = \begin{bmatrix} AL_{1,1} & AL_{1,2} & \cdots & AL_{1d} \\ AL_{2,1} & AL_{22} & \cdots & AL_{2,1} \\ \vdots & \vdots & \ddots & \vdots \\ AL_{n,1} & AL_{n,2} & \ldots & AL_{n,d} \end{bmatrix} \tag{37}$$

B. TRAPPING IN ANT LION PITS

The effects antlions' traps on the ant movement can be mathematically represented as follows:

$$L_i^t = Antlion_j^t + L_i^t \tag{38}$$

$$U_i^t = Antlion_j^t + U_i^t \tag{39}$$

C. SLIDING ANTS TOWARDS ANT LIONS

When the ants trapped in the pit of the antlion, the upper and the lower bound should reduce with the increase of iteration as follows:

$$U_i^t = \frac{U_i^t}{I} \tag{40}$$

$$L_i^t = \frac{L_i^t}{I} \tag{41}$$

where I represent a ratio that can be described as follows:

$$I = 10^{\omega} \frac{t}{T} \tag{42}$$

where T and t denote the maximum number of iterations and the current iteration. ω represents a constant which can be described as follows:

$$\omega = \begin{cases} 2t > 0.1T \\ 3t > 0.5T \\ 4t > 0.75T \\ 5t > 0.9T \\ 6t > 0.95T \end{cases} \tag{43}$$

D. ELITISM

The elitism in optimization algorithm means the best solution (best antlion) is saved as an elite, which guide the motion of the populations in the iteration process, and can be formulated as follows:

$$X_j^t = \frac{R_A^t + R_E^t}{2} \tag{44}$$

where R_A^t denotes the random walk closed to the best antlion using the roulette wheel for t-th iteration. R_E^t denotes the position of randomly walking of the j-th ant, nearby the best or the elite antlion (E) in the swarm of ants.

E. CATCHING PREY AND REBUILDING THE PIT

The final stage of hunting behavior of ant lions is catching an ant that reaches the pit's bottom. It has to update its position to the latest position by the following equation.

$$Antlion_j^t = Ant_j^t if\ f\left(Ant_j^t\right) > f\left(Antlion_j^t\right) \tag{45}$$

V. MODIFIED ANT LION OPTIMIZER (MALO)

MALO is based on enhancing the basic ALO's searching capability by enhancing the exploration and the exploitation process. The exploration phase is enhanced by applying Levy flight distribution (LFD), enabling the algorithm to jump to new areas to avoid the basic ALO's stagnation.

$$X_i^{new} = X_i + \propto \oplus Levy\left(\beta\right) \tag{46}$$

where $\propto$ represents a random step parameter; $\oplus$ respresents the entry-wise multiplication. β represents a parameter related to the LFD. The step size is described as follows:

$$\propto \oplus Levy\left(\beta\right) \sim 0.01 \frac{u}{|v|^{1/\beta}} \left(X_i^t - Antlion_j^t\right) \tag{47}$$

where u and v denote variables obtained by normal distribution as:

$$u \sim N\left(0, \phi_u^2\right), v \sim N\left(0, \phi_v^2\right) \tag{48}$$

$$\phi_u = \left[\frac{\Gamma\left(1+\beta\right) \times sin\left(\pi \times \beta/2\right)}{\Gamma\left[\left(1+\beta\right)/2\right] \times \beta}\right]^{1/\beta}, \phi_v = 1 \tag{49}$$

where Γ is the standard gamma function; $0 \leq \beta \leq 2$.

The exploitation process of the algorithm is enhanced by updating the location of ants around the elite (best) solution in a spiral path as follows:

$$X_i^{new} = \left|Antlion_j^t - X_i\right| e^{bt} \cos\left(2\pi t\right) + Antlion_j^t \tag{50}$$

b represents a constant which used for definining the logarithmic spiral shape. To balance between the exploitation and

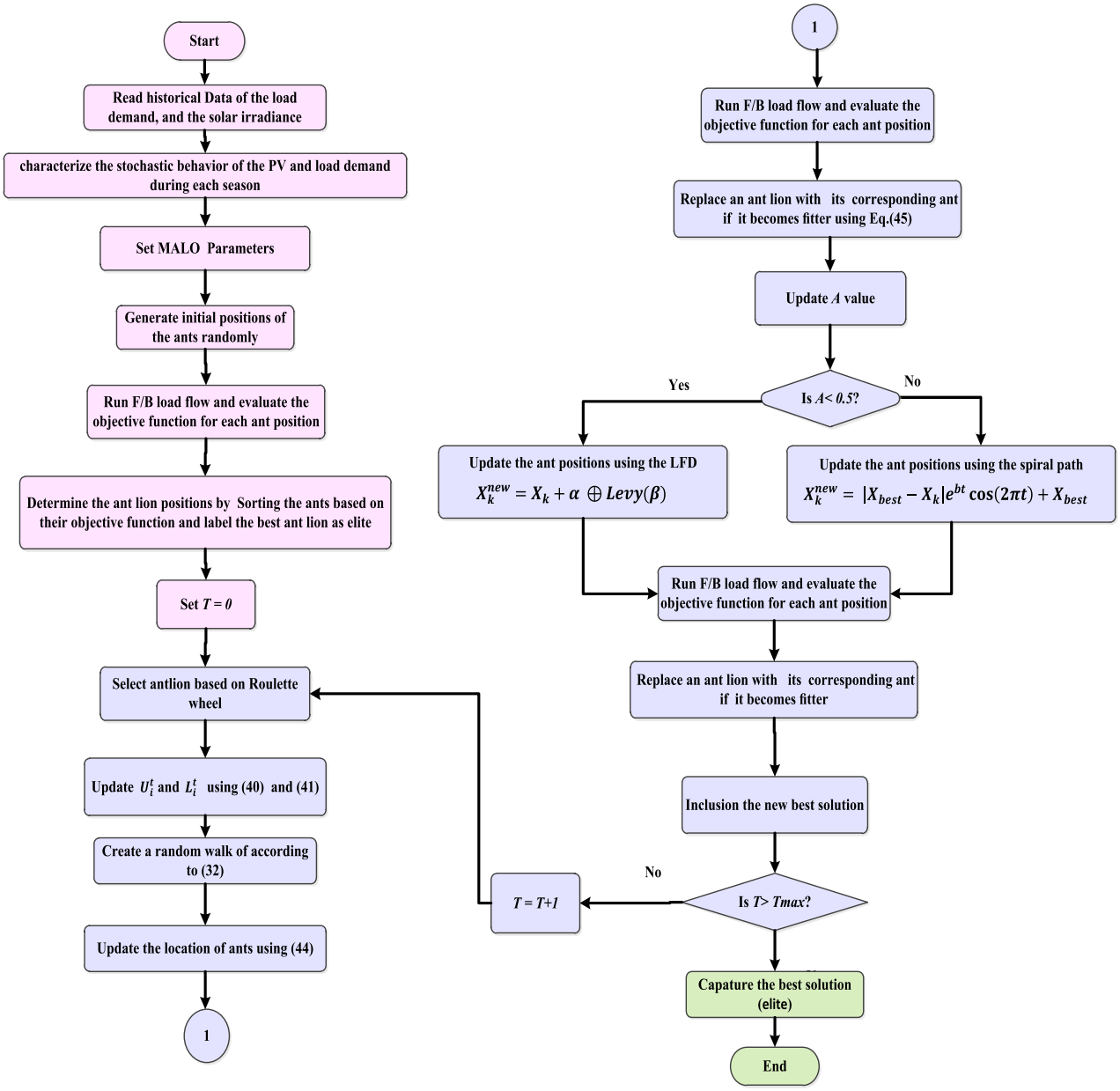

FIGURE 1. Flow chart of application of the MALO for optimal planning.

the exploration, an adaptive operator is used for this sake as depicted in the following:

$$A(t) = A_{min} + \left(\frac{A_{max} - A_{min}}{T}\right) \times t \tag{51}$$

where, A_{max} and A_{min} are the maximum and the minimum A limits. This value is changed dramatically from A_{max} to A_{min}. When the value of A is closed to A_{min}, the position of the populations will be updated using (46) for enhancing the exploration of this technique while when the value of A is closed to A_{max} the position of the populations will be updated using (50), which enhance the exploitation of this technique. The application of the proposed algorithm for solving the planning problem is depicted in Fig. 1.

VI. SIMULATION RESULTS

In this section, the proposed algorithm is applied for solving the optimal power problem for optimal allocation of a hybrid system (PV-DG and the DSTATCOM) under uncertain conditions. Two test systems are utilized to incorporate the hybrid system, which includes IEEE 69-bus and 118-bus systems. The single line diagrams of the IEEE 69-bus and 118-bus systems are depicted in Fig. 2 and Fig.3, respectively. The system's data are given in [55] and [56], respectively. The initial power flow solutions of these systems are shown in Table 1 and Table 2. The proposed technique was written using MATLAB software (MATLAB) in core I7, and 8 GB of RAM. The empirical parameters of the MALO for the studied

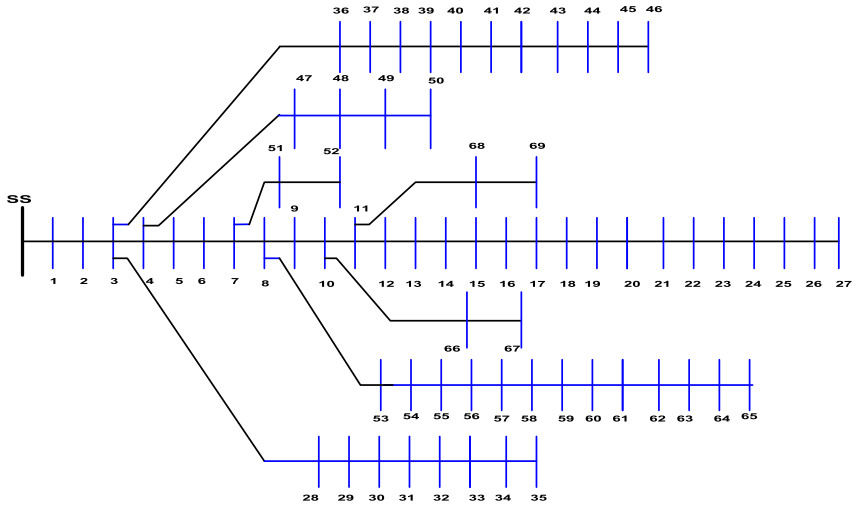

FIGURE 2. Single line diagram of the IEEE 69 bus.

TABLE 1. The system specification of 69-bus systems and its initial power flow.

Item	Value
System Specifications:	
NB	69
Npr	68
$Vsys\ (kV)$	12.66
$Base\ MVA$	100
$S_{Load}(MVA)$	3.802 + j2.694
$P_{Total_{loss}}(kW)$	225
$Q_{Total_{loss}}(kVar)$	102.198
$V_{min}\ (p.u)\ @\ bus$	0.90919, 65

TABLE 2. The system specification and initial power flow.

Item	Value
System Specifications:	
NB	118
Npr	117
$Vsys\ (kV)$	12.66
$Base\ MVA$	100
$S_{Load}(MVA)$	22.7097+ j 17.0412
$P_{Total_{loss}}(kW)$	1298.091
$Q_{Total_{loss}}(kVar)$	978.797
$V_{min}\ (p.u)\ @\ bus$	0.86880@ 77

cases are selected to be the maximum number of iterations = 100, number of populations = 25, A_{max} = 0.85 and A_{min} = 0.4. The studied cases are listed as follows:

A. CASE 1: OPTIMAL INSTALLATION OF PV SYSTEM UNDER THE DETERMINISTIC CONDITION

In this case, to state the ALO and the MALO's effectiveness, these techniques have been examined on the standard IEEE 69-bus to assign the optimal locations and ratings of the PV units for power loss minimization. Single, two, and three PV units are installed optimally, and the obtained results are compared with other reported techniques. The obtained results are listed in Table 3. Judging from this table, the power losses are reduced considerably with the increasing number of the installed PV units. Referring to the comparison of Table 4, it clear that the obtained power losses by MALO are better than ALO and the reported algorithms, which verifies the effectiveness of the proposed algorithm. The convergence characteristics of the MALO is shown in Fig. 4. This figure illustrates that the proposed algorithm has excellent and stable convergence characteristics where there is no oscillation appeared. The trends of the power losses vs. iteration number with incorporating a single DG are converged at iteration numbers 5, 15, 10 and 43 by applying the proposed method, ALO, and the modified teaching–learning-based optimization (MLBO) algorithm [57]. The trends of the power losses vs. iteration number in the case of incorporating two DGs is converged at iteration number 12, 15, 15, 35, 60, 41 using the proposed method, ALO and the modified teaching-learning based optimization (MLBO) algorithm [57], Genetic Algorithm (GA) [58], Particle Swarm Optimization (PSO) [58], and Cuckoo Search algorithm (CSA). In the case of the inclusion of three DGs, the objective function is converged at iteration number 12,23, 25 and using the proposed method, ALO, and the modified teaching-learning based optimization (MLBO) algorithm [57]. The previous comparison verified that the proposed algorithm reached to the optimal solution faster than reported algorithms.

B. CASE 2: OPTIMAL PLANNING UNDER UNCERTAINTIES OF SYSTEM

1) IEEE-69 BUS SYSTEM

In this case, the optimal planning problem is solved using the proposed algorithms under the uncertainties of the connected load and solar irradiances on IEEE 69 bus-system. The optimal planning problem is solved for a multi-objective function, including the cost reduction, the voltage profile, and stability index improvement. It should be pointed out here that three years of hourly historical data of load demand and solar irradiance have been considered in this article. Based on this, every single year has been split into four seasons. To characterize the stochastic behavior of the PV and load

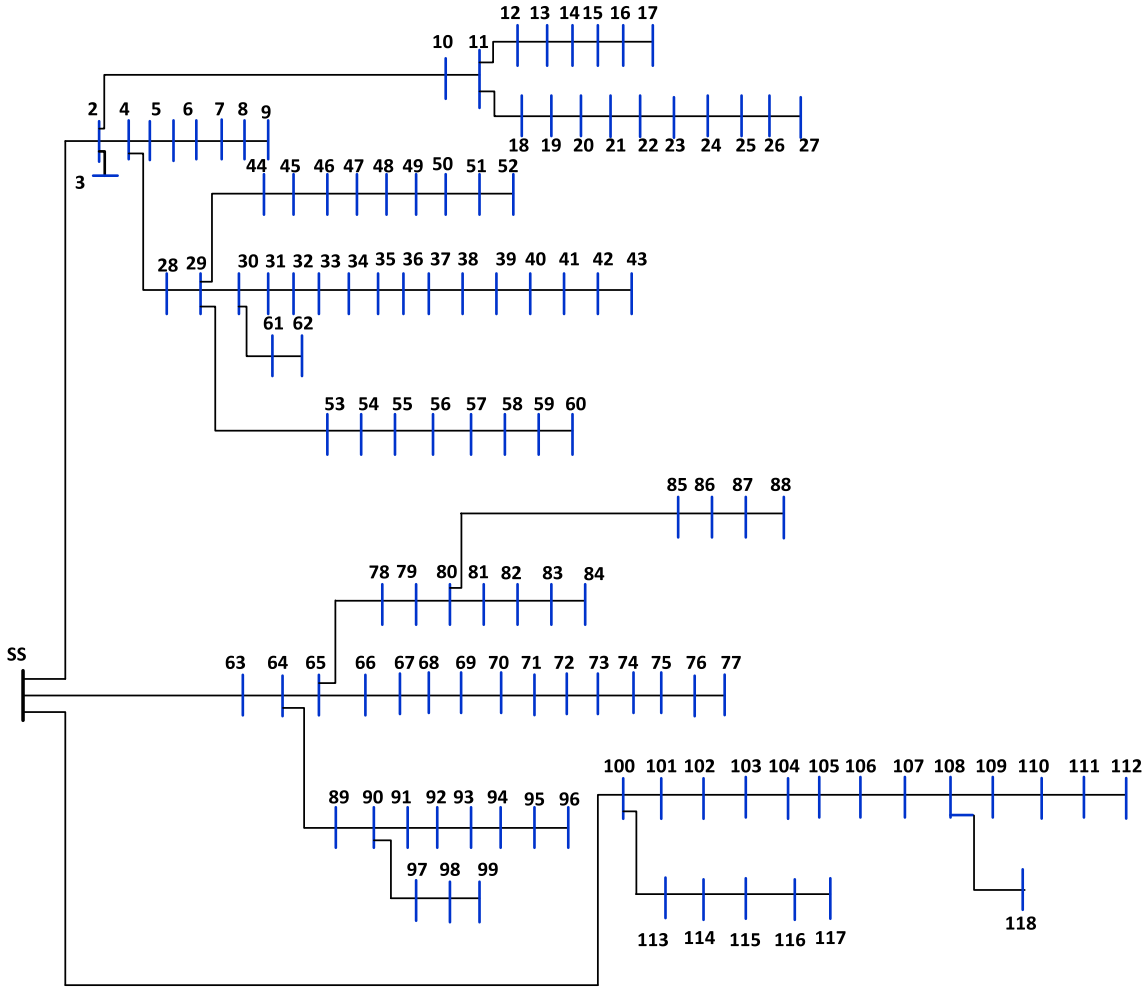

FIGURE 3. Single line diagram of the 118-bus system.

TABLE 3. Results of optimal allocation of PV units for loss reduction.

Items	Without PV	With PV					
		One PV		Two PV		Three PV	
		MALO	ALO	MALO	ALO	MALO	ALO
Total losses (kW)	225	83.222	83.222	71.674	72.518	69.426	71.714
Minimum voltage	0.9091@bus 65	0.9682@bus 27	0.9683@bus 27	0.9789@bus 65	0.9789@bus65	0.9789@bus 65	0.9789@bus 65
Maximum voltage	0.999 @ bus 2	0.999 @ bus 2	0.9999 @ bus 2	0.999 @bus 2	0.9999 @ bus 2	0.999@bus 2	1.000@ bus 40
PV size (location kW)	-	1872.7 (61)	1872.7 (61)	531.4925 (17) 1781 (61)	813.947 (12) 1735 (61)	1719.0 (61) 523 (11) 381.346 (18)	528.8338 (18) 380 (39) 1780.9 (61)
VSI (p.u)	61.2181	64.6212	64.6212	66.0295	65.7845	66.224	66.0396
VD (p.u)	1.8374	0.8729	0.8729	0.5002	0.5647	0.4504	0.4980

demand during each season, a day within that season (24 − h) is considered. Thus, each year has 96 time periods (4 seasons × 24 − h). The obtained load profiles and solar irradiance under uncertain conditions are depicted in Fig. 5 and 6.

At the base case (without the inclusion of PV or DSTATCOM), the total cost, TVD, and TVSI are 1.24867E+4 p.u, 5.48787E+5 p.u, and 2.70673E+6 $ respectively. The optimal planning problem is solved with the inclusion of single and two PV-DGs and DTSTACOMs using the proposed algorithm. The cost data of the PV-DG and the DSTATCOM are listed in Table 5. The simulation results for optimal integration of a single and two hybrid PV-DG and the DSTATCOM are listed in Table 6 and Table 7, respectively.

In case of inclusion a single hybrid system, the total cost is reduced considerably to 2.5012E+06$ or by 7.59% compared to without insertion PV-DG or DSTATCOM as well as the ***TVD*** is reduced to 6.0753E+3 p.u (51.35%) and the ***TVSI*** is enhanced to 5.7645E+5 p.u (5.04 %).

TABLE 4. Comparative results for incorporating PV in the 69-bus system.

Type	Technique	Optimal Sizes (kW)	Locations	Power loss(kW)
	Without	-	-	225
1 PV	Analytical [59]	1807.8	61	92
	Exhaustive OPF [60]	1870	61	83.23
	EA-OPF[60]	1870	61	83.23
	MTLBO[57]	1819	61	83.323
	CSA [58]	2000	61	83.8
	Hybrid method [61]	1810	61	83.372
	PSO[61]	1870	61	83.8
	GA [62]	1794	61	83.4252
	ALO	1872.7	61	83.222
	MALO	1872.7	61	83.222
2PV	MINLP[63]	510 - 1780	17 - 61	71.693
	GA [64]	1777 - 555	61 - 11	71.7912
	CSA [58]	600 - 2100	22 - 61	76.4
	GA [58]	1000 - 2400	17 - 61	82.9
	PSO [58]	700- 2100	14 - 62	78.8
	MTLBO [57]	519.705- 1732.004	17 - 61	71.776
	GA [62]	886-861	61 - 62	84.233
	ALO	813.947 - 1735	12 - 61	72.518
	MALO	531.4925 - 1781	17-61	71.674
3PV	EA[60]	467 380 1795	11 18 61	69.62
	MTLBO[57]	493 378 1672	11 18 61	69.539
	KHA [65]	496 311 1735	12 22 61	69.56
	Hybrid method [61]	510 380 1670	11 17 62	69.52
	PSO[61]	460 440 1700	11 17 61	69.541
	EA[60]	467 380 1795	11 18 61	69.62
	ALO	528.8338 380 1780.9	18 39 61	71.714
	MALO	1719.0 523 381.3461	61 11 18	69.426

Besides that, the drawn energy from the grid and the energy losses are reduced considerably. The hybrid system's assigned best location is at the 58th bus, while the size of the PV-DG and DSTATCOM are 3389kW and 2691kVAR, respectively.

The output power of the PV unit is depicted in Figure 7. It is evident that the output power of the PV unit follows the changes in the solar irradiance. Judging from Table 6, the obtained results by the proposed algorithm are better than those obtained by the conventional ALO, SCA, WOA, and GOA in terms of the cost, ***TVD***, and ***TVSI***. In this case, two-hybrid systems are embedded in the IEEE 69-bus distribution system. According to Table 7, the total cost is reduced

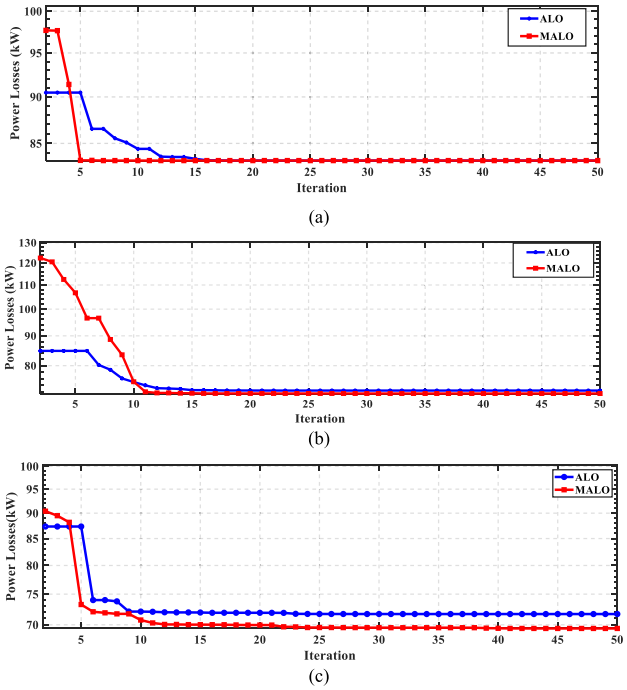

FIGURE 4. The convergence characteristic of the ALO and MALO for power loss minimization with incorporating (a) Single PV unit, (b) Two PV units, and (c) Three PV units.

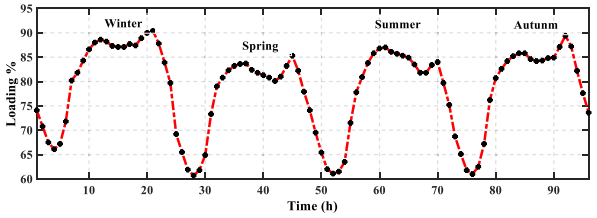

FIGURE 5. The seasonal hourly load profile.

TABLE 5. The cost coefficients of the PV-DG and the DSTATCOM.

Parameter	Value
PV Cost [66]	
C_{PV}	770 $/kW
$C_{O\&M}$	0.01 $/kWh
τ	10%
NP	20
DSTATCOM Cost [67]	
C_S	50 $/ kVAR
α	10%
ND	30
Grid Cost	
C_{loss} [68]	0.06 $/kWh
C_{Grid} [66]	0.096 $/kWh

considerably to 2.41485E+6 $ or by 10.78 % compared to the base case, and the ***TVD*** is reduced to 5.300667E+3 p.u (57.55%), and the ***TVSI*** is increased to 5.801994E+5 p.u (5.72 %). The assigned best locations of the hybrid systems for this case are at the 61st bus and the 12th bus, while the sizes of the first PV-DG and DSTATCOM are 1646 kW and 1987kVAR, respectively.

TABLE 6. The simulation results of the inclusion of single PV-DG and DSTATCOM in the 69-bus system considering the system's uncertainties.

Item	Base case	MALO	ALO	SCA	WOA	GOA
$E_{loss}(MWh)$	1.19726	1.2665	0.6582	1.2646	1.3195	1.3345
$E_{grid}(MWh)$	27.44682	21.27	24.8570	22.9680	22.6080	26.6040
Optimal Location1, Optimal Location 2	-	58	62	58	62	57
$P_{sr1}(kW)$ $P_{sr2}(kW)$	-	3389	1113	2467	2692	532
$Q_{DS1}(kVAR)$ $Q_{DS2}(kVAR)$	-	2691	1290	2694	2586	2689
TVD $(p.u)$	1.24867E+4	6.075E+3	8.736E+3	6.090E+3	6.127E+3	7.609E+3
$TVSI(p.u)$	5.487872E+5	5.76450E+5	5.62160E+5	5.7358E+5	5.75870E+5	5.66340E+5
C_{loss} ($)	7.1836199E+4	7.5988E+4	3.94910E+4	7.5876E+4	7.9171E+4	8.0073E+4
C_{Grid} ($)	2.634895E+6	2.041900E+6	2.386200E+6	2.204900E+6	2.170400E+6	2.554000E+6
C_{PV} ($)	-	3.68970E+5	1.21180E+5	2.68590E+5	2.93090E+5	5.7921E+4
C_{DS} ($)	-	1.4273E+4	6.842E+3	1.4289E+4	1.3716E+4	1.4262E+4
C_{Total} ($)	2.706731E+6	2.501200E+6	2.553700E+6	2.563600E+6	2.556300E+6	2.706200E+6

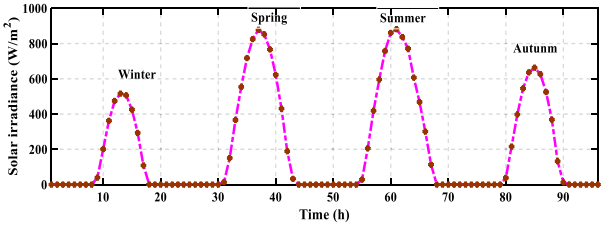

FIGURE 6. The seasons solar irradiance variations.

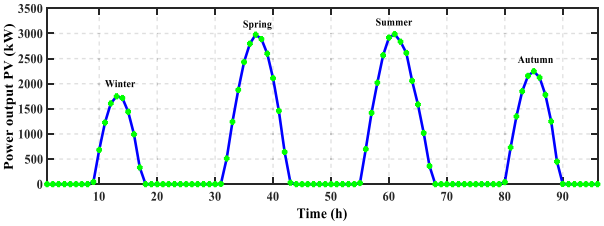

FIGURE 7. The hourly output power of the PV unit.

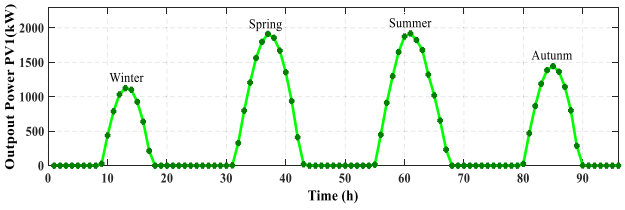

FIGURE 8. The output power of the first PV unit.

The sizes of the second PV-DG and DSTATCOM are 2155kW and 707kVAR, respectively. The first and second PV units' output power are depicted in Figures 8 and 9, respectively.

Referring to figures 8 and 9, the output power of PV units are varied during the day ahead with solar irradiance variations.

Fig. 10 shows the power losses under uncertain conditions. Referring to Fig. 10, the minimum power losses are obtained by the inclusion of two-hybrid systems. Fig. 10 the voltage profile of the system incorporating the PV-DGs and DSTATCOMs in four seasons. According to Fig. 11, it is clear

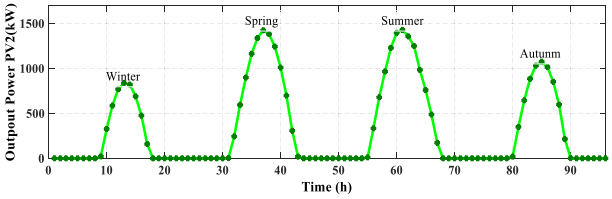

FIGURE 9. The output power of the second PV unit.

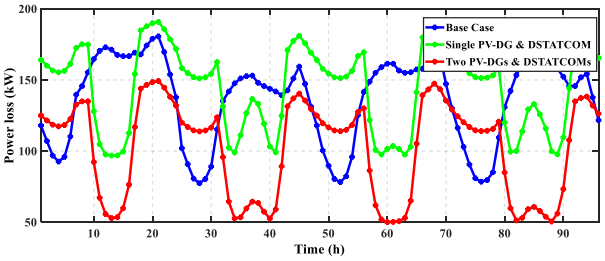

FIGURE 10. The power losses under uncertain conditions.

that the voltage profile is enhanced considerably with the inclusion of two-hybrid systems compared with the base case. Table 7 shows a comparison between the obtained results by the proposed algorithm, the conventional ALO, SCA, WOA, and GOA in terms of the cost, ***TVD***, and ***TVSI***. Judging from Table 7, the outcomes by application of the proposed algorithm are better than the reported algorithm.

2) IEEE-118 BUS SYSTEM

In this case, the proposed algorithm is applied for solving the optimal power planning problem under uncertainty conditions for the 118-bus system as a large-scale system. The system load profile and solar irradiance for this case under uncertain conditions are also depicted in Fig. 5 and Fig. 6, respectively. The optimal power planning problem solution is assessed by incorporating single and two-hybrid systems.

The outcomes for this case are listed in Table 8. At the base case (without the inclusion of PV or DSTATCOM), the total cost, ***TVD***, and ***TVSI*** are 1.61300E+7 p.u, 3.5605E+4 p.u. and 8.93320E+5 p.u., respectively. In the case of the

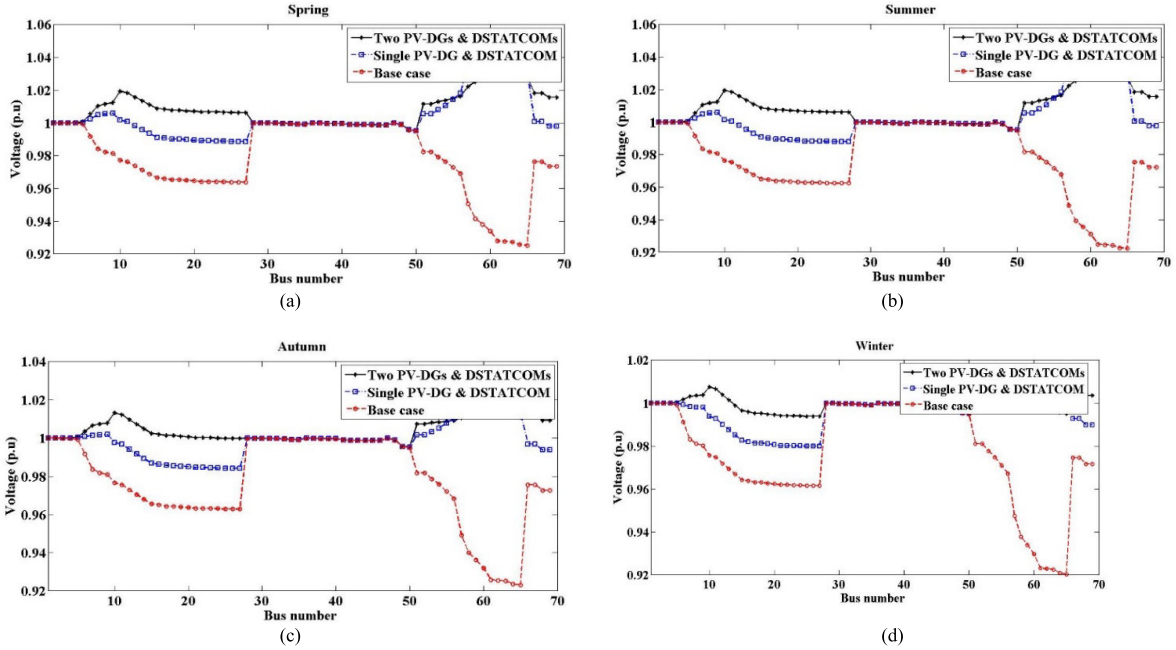

FIGURE 11. The voltage profile of the 69-bus system by incorporating the PV-DGs and DSTATCOMs in (a) Spring, (b) Summer, (c)Autumn (d) Winter.

TABLE 7. The simulation results of the inclusion of two PV-DGs and DSTATCOMs in the 69-bus system considering the system's uncertainties.

Item	MALO	ALO	SCA	WOA	GOA
$E_{loss}(MWh)$	0.892426	0.8136	1.3468	1.0280	1.1174
$E_{grid}(MWh)$	20.137	23.3281	21.2413	21.5289	21.6146
Optimal Location1,	61	63	57	63	62
Optimal Location 2	12	57	61	59	58
$P_{sr1}(kW)$	1646	690	3018	1868	1805
$P_{sr2}(kW)$	2155	1337	429	1251	1316
$Q_{DS1}(kVAR)$	1987	1449	159	1163	935
$Q_{DS2}(kVAR)$	707	581	2503	1241	1683
TVD $(p.u)$	5.301E+3	6.949E+3	5.855E+3	6.333E+3	6.118E+3
$TVSI(p.u)$	5.80198E+5	5.68974E+5	5.76828E+5	5.75773E+5	5.76570E+5
C_{loss} ($)	5.3545E+4	4.8816E+4	8.0808E+4	6.1681E+4	6.70425E+4
C_{Grid} ($)	1.93319E+6	2.23950E+6	2.03916E+6	2.06677E+6	2.07501E+6
C_{PV} ($)	4.13822E+5	2.20680E+5	3.75311E+5	3.39581E+5	3.39798E+5
C_{DS} ($)	1.4288E+4	1.0767E+4	1.4119E+4	1.2750E+4	1.3885E+4
C_{Total} ($)	2.414851E+6	2.519764E+6	2.50940E+6	2.48078E+6	2.49573E+6

TABLE 8. The simulation results of the inclusion of the PV-DGs and DSTATCOMs in the 118-bus system considering the system's uncertainties.

Item	Base case	Single hybrid system		Two hybrid system	
		ALO	MALO	ALO	MALO
$E_{loss}(MWh)$	6.8999	7.9161	7.7761	7.7213	7.1755
$E_{grid}(MWh)$	163.7100	151.3400	122.7400	138.4801	122.1273
Optimal Location1,	-	64	64	65	65
Optimal Location 2				22	30
$P_{sr1}(kW)$	-	7266	22709	10795	3498
$P_{sr2}(kW)$				3338	18177
$Q_{DS1}(kVAR)$	-	16030	14642	10072	12676
$Q_{DS2}(kVAR)$				2300	9308
TVD $(p.u)$	3.5605E+4	2.5614E+4	2.5869E+4	2.4357E+4	2.1244E+4
$TVSI(p.u)$	8.93320E+5	9.33530E+5	9.34980E+5	9.40625E+5	9.51969E+5
C_{loss} ($)	4.13990E+5	4.74970E+5	4.66570E+5	4.63276E+5	4.30531E+5
C_{Grid} ($)	1.57160E+7	1.45280E+7	1.17830E+7	1.32941E+7	1.17242E+7
C_{PV} ($)	-	7.9107E+5	2.4724E+6	1.5388E+6	2.4722E+6
C_{DS} ($)	-	8.5023E+4	7.7661E+4	5.3421E+4	2.7013E+4
C_{Total} ($)	1.61300E+7	1.58790E+7	1.47990E+7	1.53496E+7	1.465397E+7

inclusion a single PV-DG and DSTATCOM, the total cost and the ***TVD*** are reduced to 1.47990E+7 $ and 2.5869E+4 p.u., respectively. While the ***TVSI*** is enhanced to 9.34980E+5 p.u. The hybrid system's optimal location is at bus number 64,

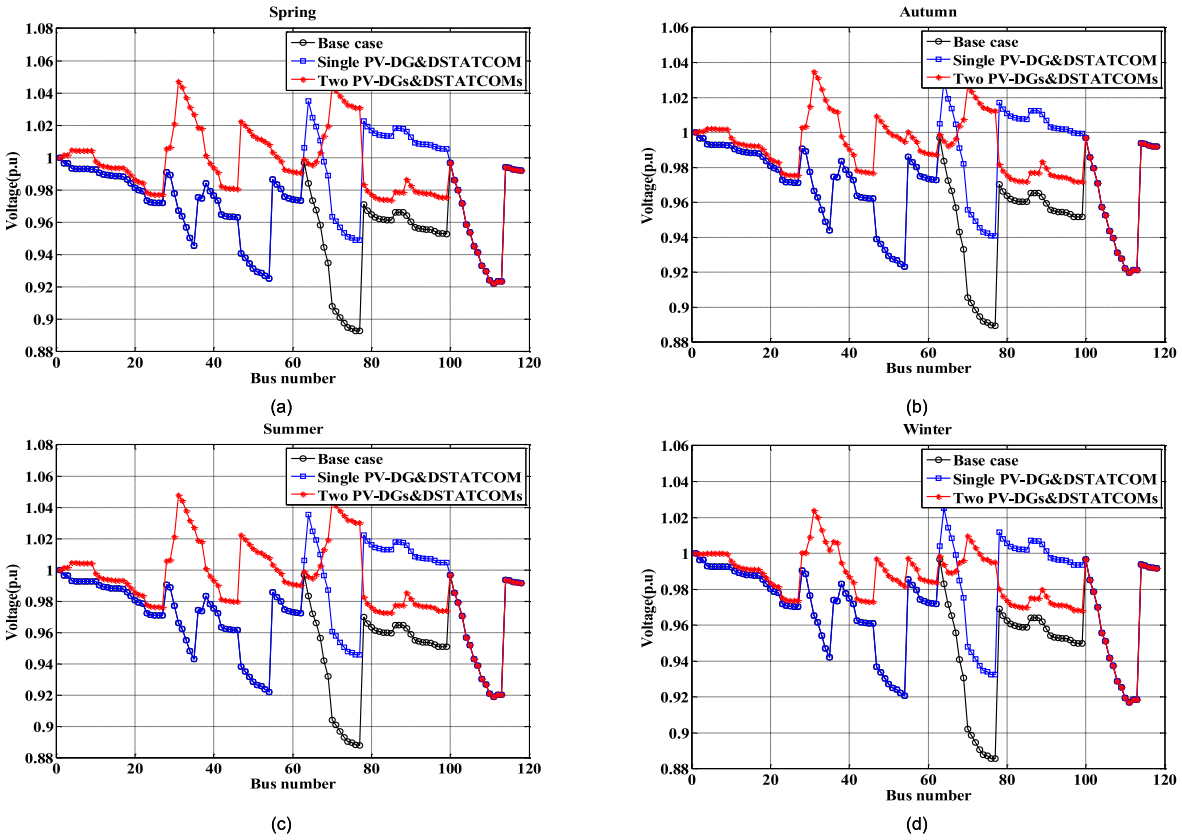

FIGURE 12. The voltage profile of 118-bus system by incorporating the PV-DGs and DSTATCOMs in (a) Spring, (b) Summer, (c)Autumn (d) Winter.

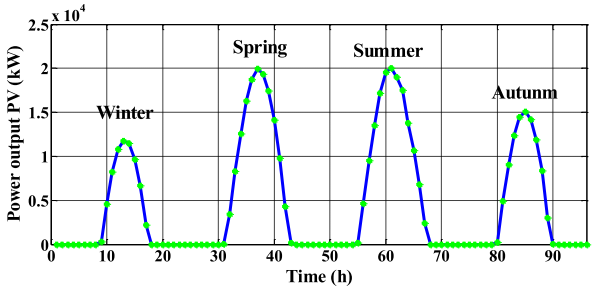

FIGURE 13. The hourly output power of the single PV unit in the 118-bus system.

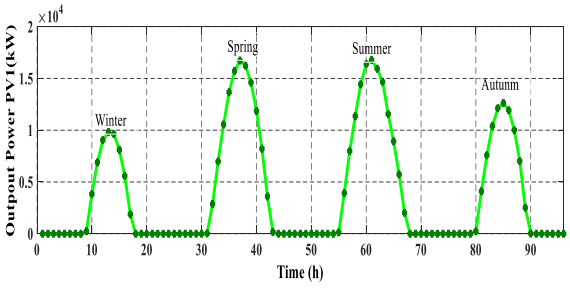

FIGURE 14. The output power of the first PV unit in the 118-bus system.

while the optimal ratings of the PV-DG and DSTATCOM are 22709 kW and 14642 kVAR, respectively. The voltage profile for this is illustrated in Fig. 12. From this figure, the voltage

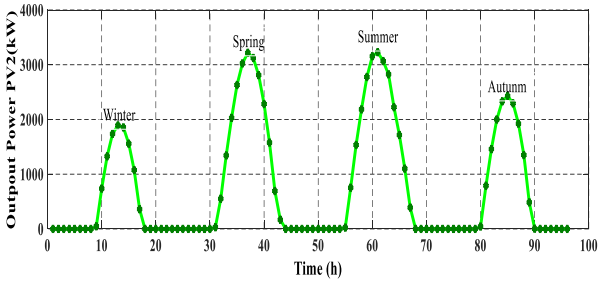

FIGURE 15. The output power of the second PV unit in the 118-bus system.

profile is enhanced with the inclusion a single PV-DG and DSTATCOM.The output power of the PV unit for this case is depicted in Fig. 11. According to this figure the output power is changed hourly with variations of the solar irradiance. In case of incorporating two PV-DGs and DSTATCOMs in system, the total cost and the system performance is enhanced considerably where the total cost and the ***TVD*** are reduced to 1.465397E+7 $ and 2.1244E+4 p.u. respectively. While the ***TVSI*** is enhanced to 9.51969E+5p.u.

VII. CONCLUSION

In this study, the optimal planning and assessment of integration a hybrid system including PV- DG and DSTATCOM have been addressed considering the seasonal variations of

the load demand and the solar irradiance. The stochastic nature of load demand and the solar irradiance are correctly modeled using normal and Beta probability density functions. A modified Ant lion optimizer (MALO) has been proposed based on the Levy Flight Distribution and spiral orientation movement of the populations to improve the conventional ALO searching abilities. The proposed MALO applied to assign the optimal site and size of a multi-objective function has been considered, including the cost reduction, the voltage profile, and stability index improvement. The proposed method has been implemented on IEEE 69-bus and 118-bus systems. A comparison for power loss minimization at deterministic conditions has been carried out to verify the proposed technique's effectiveness.

The simulation results reveal the following conclusions:

- The proposed MALO enables a robust and powerful tool for optimal planning of PV-DG and DSTATCOM in the distribution system.
- The proposed MALO is superior for loss reduction compared with the state-of-the-art algorithms.
- Optimal incorporating a single hybrid PV-DG and DSTATCOM in the 69-bus system can minimize the total annual cost, the voltage deviations by 7.59 % and 51.35 %, respectively. The voltage stability is enhanced by 5.05 %compared with the base case while optimal incorporating two-hybrid PV-DG and DSTATCOM can minimize the total annual cost, the voltage deviations by 10.78 % 57.55%, respectively. Also, the voltage stability is enhanced by 5.72 % compared with the base case.
- In optimal incorporation, a single hybrid PV-DG and DSTATCOM in the 118-bus system can minimize the expected cost, the voltage deviations by 8.25 % and 27.34 %, respectively. The voltage stability is enhanced by 4.66 %compared with the base case, while optimal incorporating of two hybrid PV-DG and DSTATCOM can minimize the total annual cost, the voltage deviations by 9.151 % and 40.33 %, respectively. Also, the voltage stability is enhanced by 6.57 % compared with the base case.

The future work related to optimal integration of PV-DG and DSTATCOM is solving the optimal power planning problem by considering multi types of energy storage systems such as batteries, hydro pump, compressed air, Fuel cell, and superconducting magnetic energy storage. Besides that, solving this problem in the presence of the plug-in vehicles.

REFERENCES

[1] M. F. Akorede, H. Hizam, and E. Pouresmaeil, "Distributed energy resources and benefits to the environment," *Renew. Sustain. Energy Rev.*, vol. 14, no. 2, pp. 724–734, Feb. 2010.

[2] A. R. Gupta and A. Kumar, "Deployment of distributed generation with D-FACTS in distribution system: A comprehensive analytical review," *IETE J. Res.*, pp. 1–18, Jul. 2019.

[3] M. Ebeed, S. Kamel, S. H. A. Aleem, and A. Y. Abdelaziz, "Optimal allocation of compensators," in *Electric Distribution Network Planning*. Springer, 2018, pp. 321–353.

[4] R. O. Bawazir and N. S. Cetin, "Comprehensive overview of optimizing PV-DG allocation in power system and solar energy resource potential assessments," *Energy Rep.*, vol. 6, pp. 173–208, Nov. 2020.

[5] S. Jazebi, S. H. Hosseinian, and B. Vahidi, "DSTATCOM allocation in distribution networks considering reconfiguration using differential evolution algorithm," *Energy Convers. Manage.*, vol. 52, no. 7, pp. 2777–2783, Jul. 2011.

[6] O. P. Mahela and A. G. Shaik, "Power quality improvement in distribution network using DSTATCOM with battery energy storage system," *Int. J. Electr. Power Energy Syst.*, vol. 83, pp. 229–240, Dec. 2016.

[7] S. A. Taher and S. A. Afsari, "Optimal location and sizing of DSTATCOM in distribution systems by immune algorithm," *Int. J. Electr. Power Energy Syst.*, vol. 60, pp. 34–44, Sep. 2014.

[8] T. Yuvaraj, K. R. Devabalaji, and K. Ravi, "Optimal placement and sizing of DSTATCOM using harmony search algorithm," *Energy Procedia*, vol. 79, pp. 759–765, Nov. 2015.

[9] N. Salman, A. Mohamed, and H. Shareef, "Reliability improvement in distribution systems by optimal placement of DSTATCOM using binary gravitational search algorithm," *Przeglad Elektrotechniczny*, vol. 88, no. 2, pp. 295–299, 2012.

[10] M. Sedighizadeh and A. Eisapour-Moarref, "The imperialist competitive algorithm for optimal multi-objective location and sizing of DSTATCOM in distribution systems considering loads uncertainty," *INAE Lett.*, vol. 2, no. 3, pp. 83–95, Sep. 2017.

[11] D. K. Rukmani, Y. Thangaraj, U. Subramaniam, S. Ramachandran, R. M. Elavarasan, N. Das, L. Baringo, and M. I. A. Rasheed, "A new approach to optimal location and sizing of DSTATCOM in radial distribution networks using bio-inspired cuckoo search algorithm," *Energies*, vol. 13, no. 18, p. 4615, Sep. 2020.

[12] P. Balamurugan, T. Yuvaraj, and P. Muthukannan, "Optimal allocation of DSTATCOM in distribution network using whale optimization algorithm," *Eng., Technol. Appl. Sci. Res.*, vol. 8, no. 5, pp. 3445–3449, Oct. 2018.

[13] J. Sanam, "Optimization of planning cost of radial distribution networks at different loads with the optimal placement of distribution STATCOM using differential evolution algorithm," *Soft Comput.*, vol. 24, pp. 13269–13284, Sep. 2020.

[14] A. Selim, S. Kamel, and F. Jurado, "Optimal allocation of distribution static compensators using a developed multi-objective sine cosine approach," *Comput. Electr. Eng.*, vol. 85, Jul. 2020, Art. no. 106671.

[15] M. Mohammadi, M. Abasi, and A. M. Rozbahani, "Fuzzy-GA based algorithm for optimal placement and sizing of distribution static compensator (DSTATCOM) for loss reduction of distribution network considering reconfiguration," *J. Central South Univ.*, vol. 24, no. 2, pp. 245–258, Feb. 2017.

[16] H. B. Tolabi, M. H. Ali, and M. Rizwan, "Simultaneous reconfiguration, optimal placement of DSTATCOM, and photovoltaic array in a distribution system based on fuzzy-ACO approach," *IEEE Trans. Sustain. Energy*, vol. 6, no. 1, pp. 210–218, Jan. 2015.

[17] S. Devi and M. Geethanjali, "Optimal location and sizing determination of distributed generation and DSTATCOM using particle swarm optimization algorithm," *Int. J. Electr. Power Energy Syst.*, vol. 62, pp. 562–570, Nov. 2014.

[18] K. R. Devabalaji and K. Ravi, "Optimal size and siting of multiple DG and DSTATCOM in radial distribution system using bacterial foraging optimization algorithm," *Ain Shams Eng. J.*, vol. 7, no. 3, pp. 959–971, Sep. 2016.

[19] Y. Thangaraj and R. Kuppan, "Multi-objective simultaneous placement of DG and DSTATCOM using novel lightning search algorithm," *J. Appl. Res. Technol.*, vol. 15, no. 5, pp. 477–491, Oct. 2017.

[20] S. R. Ghatak, S. Sannigrahi, and P. Acharjee, "Optimised planning of distribution network with photovoltaic system, battery storage, and DSTATCOM," *IET Renew. Power Gener.*, vol. 12, no. 15, pp. 1823–1832, Nov. 2018.

[21] T. Yuvaraj, K. R. Devabalaji, and S. B. Thanikanti, "Simultaneous allocation of DG and DSTATCOM using whale optimization algorithm," *Iranian J. Sci. Technol., Trans. Electr. Eng.*, vol. 44, no. 2, pp. 879–896, Jun. 2020.

[22] S. G. R. Chinnaraj and R. Kuppan, "Optimal sizing and placement of multiple renewable distribution generation and DSTATCOM in radial distribution systems using hybrid lightning search algorithm-simplex method optimization algorithm," *Comput. Intell.*, to be published.

[23] A. Selim, S. Kamel, A. S. Alghamdi, and F. Jurado, "Optimal placement of DGs in distribution system using an improved harris hawks optimizer based on single- and multi-objective approaches," *IEEE Access*, vol. 8, pp. 52815–52829, 2020.

[24] K. Zou, A. P. Agalgaonkar, K. M. Muttaqi, and S. Perera, "Distribution system planning with incorporating DG reactive capability and system uncertainties," *IEEE Trans. Sustain. Energy*, vol. 3, no. 1, pp. 112–123, Jan. 2012.

[25] Z. Liu, F. Wen, and G. Ledwich, "Optimal siting and sizing of distributed generators in distribution systems considering uncertainties," *IEEE Trans. Power Del.*, vol. 26, no. 4, pp. 2541–2551, Oct. 2011.

[26] M. Ebeed, A. Alhejji, S. Kamel, and F. Jurado, "Solving the optimal reactive power dispatch using marine predators algorithm considering the uncertainties in load and wind-solar generation systems," *Energies*, vol. 13, no. 17, p. 4316, Aug. 2020.

[27] M. Ebeed, A. Ali, M. I. Mosaad, and S. Kamel, "An improved lightning attachment procedure optimizer for optimal reactive power dispatch with uncertainty in renewable energy resources," *IEEE Access*, vol. 8, pp. 168721–168731, 2020.

[28] S. Abdel-Fatah, M. Ebeed, S. Kamel, and J. Yu, "Reactive power dispatch solution with optimal installation of renewable energy resources considering uncertainties," in *Proc. IEEE Conf. Power Electron. Renew. Energy (CPERE)*, Oct. 2019, pp. 118–123.

[29] M. M. Ansari, C. Guo, M. Shaikh, N. Chopra, B. Yang, J. Pan, Y. Zhu, and X. Huang, "Considering the uncertainty of hydrothermal wind and solar-based DG," *Alexandria Eng. J.*, vol. 59, no. 6, pp. 4211–4236, Dec. 2020.

[30] M. Khajevand, A. Fakharian, and M. Sedighizadeh, "Stochastic joint optimal distributed generation scheduling and distribution feeder reconfiguration of microgrids considering uncertainties modeled by copula-based method," *Iranian J. Electr. Electron. Eng.*, vol. 16, no. 3, pp. 371–392, 2020.

[31] L. Luo, S. S. Abdulkareem, A. Rezvani, M. R. Miveh, S. Samad, N. Aljojo, and M. Pazhoohesh, "Optimal scheduling of a renewable based microgrid considering photovoltaic system and battery energy storage under uncertainty," *J. Energy Storage*, vol. 28, Apr. 2020, Art. no. 101306.

[32] S. Kamel, A. Ramadan, M. Ebeed, L. Nasrat, and M. H. Ahmed, "Sizing and evaluation analysis of hybrid solar-wind distributed generations in real distribution network considering the uncertainty," in *Proc. Int. Conf. Comput., Control, Electr., Electron. Eng. (ICCCEEE)*, Sep. 2019, pp. 1–5.

[33] A. Ramadan, M. Ebeed, S. Kamel, and L. Nasrat, "Optimal allocation of renewable energy resources considering uncertainty in load demand and generation," in *Proc. IEEE Conf. Power Electron. Renew. Energy (CPERE)*, Oct. 2019, pp. 124–128.

[34] A. Ahmed, M. F. Nadeem, I. A. Sajjad, R. Bo, I. A. Khan, and A. Raza, "Probabilistic generation model for optimal allocation of wind DG in distribution systems with time varying load models," *Sustain. Energy, Grids Netw.*, vol. 22, Jun. 2020, Art. no. 100358.

[35] S. Mirjalili, "The ant lion optimizer," *Adv. Eng. Softw.*, vol. 83, pp. 80–98, May 2015.

[36] A. A. Heidari, H. Faris, S. Mirjalili, I. Aljarah, and M. Mafarja, "Ant lion optimizer: Theory, literature review, and application in multi-layer perceptron neural networks," in *Nature-Inspired Optimizers*. Springer, 2020, pp. 23–46.

[37] A. S. Assiri, A. G. Hussien, and M. Amin, "Ant lion optimization: Variants, hybrids, and applications," *IEEE Access*, vol. 8, pp. 77746–77764, 2020.

[38] Z. Wu, D. Yu, and X. Kang, "Parameter identification of photovoltaic cell model based on improved ant lion optimizer," *Energy Convers. Manage.*, vol. 151, pp. 107–115, Nov. 2017.

[39] M. Wang, C. Wu, L. Wang, D. Xiang, and X. Huang, "A feature selection approach for hyperspectral image based on modified ant lion optimizer," *Knowl.-Based Syst.*, vol. 168, pp. 39–48, Mar. 2019.

[40] M. M. Mafarja and S. Mirjalili, "Hybrid binary ant lion optimizer with rough set and approximate entropy reducts for feature selection," *Soft Comput.*, vol. 23, no. 15, pp. 6249–6265, Aug. 2019.

[41] S. K. Dinkar and K. Deep, "Opposition based Laplacian ant lion optimizer," *J. Comput. Sci.*, vol. 23, pp. 71–90, Nov. 2017.

[42] K. Zhang, J. Ma, X. Zhao, X. Liu, and Y. Zhang, "Parameter identification and state of charge estimation of NMC cells based on improved ant lion optimizer," *Math. Problems Eng.*, vol. 2019, pp. 1–18, Jul. 2019.

[43] S. K. Dinkar and K. Deep, "An efficient opposition based Lévy flight antlion optimizer for optimization problems," *J. Comput. Sci.*, vol. 29, pp. 119–141, Nov. 2018.

[44] H. M. Zawbaa, E. Emary, and C. Grosan, "Feature selection via chaotic antlion optimization," *PLoS ONE*, vol. 11, no. 3, Mar. 2016, Art. no. e0150652.

[45] Q. Sun, R. Han, H. Zhang, J. Zhou, and J. M. Guerrero, "A multiagent-based consensus algorithm for distributed coordinated control of distributed generators in the energy Internet," *IEEE Trans. Smart Grid*, vol. 6, no. 6, pp. 3006–3019, Nov. 2015.

[46] W. Rui, S. Qiuye, M. Dazhong, and H. Xuguang, "Line impedance cooperative stability region identification method for grid-tied inverters under weak grids," *IEEE Trans. Smart Grid*, vol. 11, no. 4, pp. 2856–2866, Jul. 2020.

[47] S. Barshandeh and M. Haghzadeh, "A new hybrid chaotic atom search optimization based on tree-seed algorithm and Levy flight for solving optimization problems," *Eng. Comput.*, pp. 1–44, Feb. 2020.

[48] R. Zhao, Y. Wang, C. Liu, P. Hu, Y. Li, H. Li, and C. Yuan, "Selfish herd optimizer with Levy-flight distribution strategy for global optimization problem," *Phys. A, Stat. Mech. Appl.*, vol. 538, Jan. 2020, Art. no. 122687.

[49] Y. Liu and B. Cao, "A novel ant colony optimization algorithm with Levy flight," *IEEE Access*, vol. 8, pp. 67205–67213, 2020.

[50] S. Chhikara and R. Kumar, "MI-LFGOA: Multi-island levy-flight based grasshopper optimization for spatial image steganalysis," *Multimedia Tools Appl.*, vol. 79, nos. 39–40, pp. 29723–29750, Oct. 2020.

[51] R. Pal and M. Saraswat, "Histopathological image classification using enhanced bag-of-feature with spiral biogeography-based optimization," *Int. J. Speech Technol.*, vol. 49, no. 9, pp. 3406–3424, Sep. 2019.

[52] M. A. Taher, S. Kamel, F. Jurado, and M. Ebeed, "Modified grasshopper optimization framework for optimal power flow solution," *Electr. Eng.*, vol. 101, no. 1, pp. 121–148, Apr. 2019.

[53] M. Guo, J.-S. Wang, L. Zhu, S. Guo, and W. Xie, "Improved ant lion optimizer based on spiral complex path searching patterns," *IEEE Access*, vol. 8, pp. 22094–22126, 2020.

[54] R. H. A. Zubo, G. Mokryani, and R. Abd-Alhameed, "Optimal operation of distribution networks with high penetration of wind and solar power within a joint active and reactive distribution market environment," *Appl. Energy*, vol. 220, pp. 713–722, Jun. 2018.

[55] N. C. Sahoo and K. Prasad, "A fuzzy genetic approach for network reconfiguration to enhance voltage stability in radial distribution systems," *Energy Convers. Manage.*, vol. 47, nos. 18–19, pp. 3288–3306, Nov. 2006.

[56] D. Zhang, Z. Fu, and L. Zhang, "An improved TS algorithm for loss-minimum reconfiguration in large-scale distribution systems," *Electric Power Syst. Res.*, vol. 77, nos. 5–6, pp. 685–694, Apr. 2007.

[57] J. A. M. García and A. J. G. Mena, "Optimal distributed generation location and size using a modified teaching–learning based optimization algorithm," *Int. J. Electr. Power Energy Syst.*, vol. 50, pp. 65–75, Sep. 2013.

[58] W. S. Tan, M. Y. Hassan, M. S. Majid, and H. A. Rahman, "Allocation and sizing of DG using cuckoo search algorithm," in *Proc. IEEE Int. Conf. Power Energy (PECon)*, Dec. 2012, pp. 133–138.

[59] N. Acharya, P. Mahat, and N. Mithulananthan, "An analytical approach for DG allocation in primary distribution network," *Int. J. Electr. Power Energy Syst.*, vol. 28, no. 10, pp. 669–678, Dec. 2006.

[60] K. Mahmoud, N. Yorino, and A. Ahmed, "Optimal distributed generation allocation in distribution systems for loss minimization," *IEEE Trans. Power Syst.*, vol. 31, no. 2, pp. 960–969, Mar. 2016.

[61] S. Kansal, V. Kumar, and B. Tyagi, "Hybrid approach for optimal placement of multiple DGs of multiple types in distribution networks," *Int. J. Electr. Power Energy Syst.*, vol. 75, pp. 226–235, Feb. 2016.

[62] I. Pisica, C. Bulac, and M. Eremia, "Optimal distributed generation location and sizing using genetic algorithms," in *Proc. 15th Int. Conf. Intell. Syst. Appl. to Power Syst.*, Nov. 2009, pp. 1–6.

[63] S. Kaur, G. Kumbhar, and J. Sharma, "A MINLP technique for optimal placement of multiple DG units in distribution systems," *Int. J. Electr. Power Energy Syst.*, vol. 63, pp. 609–617, Dec. 2014.

[64] T. N. Shukla, S. P. Singh, V. Srinivasarao, and K. B. Naik, "Optimal sizing of distributed generation placed on radial distribution systems," *Electr. Power Compon. Syst.*, vol. 38, no. 3, pp. 260–274, Jan. 2010.

[65] S. Kamel, A. Amin, A. Selim, and M. H. Ahmed, "Optimal placement of DG and capacitor in radial distribution systems considering load variation," in *Proc. Int. Conf. Comput., Control, Electr., Electron. Eng. (ICCCEEE)*, Sep. 2019, pp. 1–6.

[66] S. R. Gampa and D. Das, "Optimum placement and sizing of DGs considering average hourly variations of load," *Int. J. Electr. Power Energy Syst.*, vol. 66, pp. 25–40, Mar. 2015.

[67] A. R. Gupta and A. Kumar, "Performance analysis of radial distribution systems with UPQC and D-STATCOM," *J. Inst. Eng. (India), Ser. B*, vol. 98, no. 4, pp. 415–422, Aug. 2017.

[68] S. Sultana and P. K. Roy, "Optimal capacitor placement in radial distribution systems using teaching learning based optimization," *Int. J. Electr. Power Energy Syst.*, vol. 54, pp. 387–398, Jan. 2014.